Further reading

A very large number of papers have appeared in the literature that calculate the transmission properties of small conductors. We have cited a few papers in the text that should provide a citation trail for the interested reader. The very brief introduction to Green's functions in Section 3.3 can be supplemented with standard texts such as

[3.1] Inkson, J. C. (1984), *Many-body Theory of Solids*, (New York, Plenum). See Chapter 2.

[3.2] Economou, E. N. (1983), *Green's Functions in Quantum Physics*, Springer Series in Solid-state Sciences, vol.7, (Heidelberg, Springer–Verlag).

[3.3] Schiff L. I. (1968). *Quantum Mechanics*, Chapter 9, Third Edition, (New York, McGraw–Hill).

Quantum Hall effect

One of the most significant discoveries of the 1980s is the quantum Hall effect (see K. von Klitzing, G. Dorda and M. Pepper (1980), *Phys. Rev. Lett.*, **45**, 494). Normally in solid state experiments, scattering processes introduce enough uncertainty that most results have an 'error bar' of plus or minus several per cent. For example, the conductance of a ballistic conductor has been shown (see Fig. 2.1.2) to be quantized in units of $(h/2e^2)$. But this is true as long as we are not bothered by deviations of a few per cent, since real conductors are usually not precisely ballistic. On the other hand, at high magnetic fields the Hall resistance has been observed to be quantized in units of $(h/2e^2)$ with an accuracy that is specified in parts per million. Indeed the accuracy of the quantum Hall effect is so impressive that the National Institute of Standards and Technology is interested in utilizing it as a resistance standard.

This impressive accuracy arises from the near complete suppression of momentum relaxation processes in the quantum Hall regime resulting in a truly ballistic conductor of incredibly high quality. Mean free paths of several millimeters have been observed. These unusually long mean free paths do not arise from any unusual purity of the samples. They arise because, at high magnetic fields, the electronic states carrying current in one direction are localized on one side of the sample while those carrying current in the other direction are localized on the other side of the sample. Due to the formation of this 'divided highway' there is hardly any overlap between the two groups of states and backscattering cannot take place even though impurities are present.

that lead to zero longitudinal resistance and consequently the quantization of the Hall resistance. We then discuss (Section 4.2) some of the surprising experiments in the quantum Hall regime reported in the late 1980s where controlled amounts of backscattering are deliberately introduced.

4.1 Origin of 'zero' resistance

We know that at high magnetic fields the longitudinal resistance (measured using a macroscopic Hall bridge) oscillates as a function of the magnetic field (see Fig. 1.4.2). As we discussed in Section 1.5 the density of states at high magnetic fields develops sharp peaks spaced by $\hbar\omega_c$ (see Fig. 1.5.1) and the resistivity oscillates as the position of these peaks is changed relative to the Fermi energy. This can be done either by changing the magnetic field as shown in Fig. 1.4.2 or by keeping the magnetic field fixed and changing the electron density (and hence the Fermi energy) by means of a gate voltage. Indeed the first experiment reporting the quantum Hall effect was performed on a silicon inversion layer as a function of the gate voltage at a magnetic field of B = 18 T.

Intuitively it might appear that the resistance should be a minimum whenever the Fermi energy coincides with a peak in the density of states, that is, with a Landau level. However, the correct answer is just the opposite. The resistance is a minimum when the Fermi energy lies between two Landau levels so that the density of states at the Fermi energy is a minimum! But how does a sample carry any current unless there are states at the Fermi energy? The answer is that there are states at the Fermi energy which are located near the edges of the sample. Normally in wide conductors we tend to ignore the edges since they form an insignificant fraction of the entire conductor. But these *edge states* play a very important role in carrying the current at the resistance minimum as discussed by several authors (see, for example, B. I. Halperin (1982), *Phys. Rev. B*, **25**, 2185, and A. H. MacDonald and P. Streda (1984), *Phys. Rev. B*, **29**, 1616). This is reminiscent of the boundary problems encountered in calculating the diamagnetism of a free electron gas (see Section 4.3 of R. Peierls (1979), *Surprises in Theoretical Physics*, Princeton University Press).

An important point to note from Fig. 1.4.2 is that at the minima the resistance is very nearly zero. This is particularly surprising since the resistance is so close to zero shows that the electrons are able to travel such huge distances without losing their momentum. Clearly something rather special must be happening at the microscopic level leading to this fantastic suppression of momentum relaxation processes.

We have already seen in Section 1.6 that as we increase the magnetic field in a finite-width conductor, the states carrying current in one direction get spatially separated from the states carrying current in the opposite direction. The result is a significant reduction in the spatial overlap between the forward and the backward propagating states which leads to a suppression of backscattering (and hence momentum relaxation). Indeed at high magnetic fields the forward and backward propagating states are spatially separated by the width of the conductor and thus have practically zero overlap in wide conductors.

In Section 1.6 we assumed a parabolic confining potential $U(y) = m\omega_0^2 y^2/2$. This allowed us to obtain the eigenfunctions of the Schrödinger equation (see Eq.(1.2.2))

$$\left[E_s + \frac{(i\hbar\nabla + e\mathbf{A})^2}{2m} + U(y)\right]\Psi(x,y) = E\Psi(x,y) \qquad (4.1.1)$$

analytically. A parabolic potential often provides a good description of narrow quantum wires. But for wide conductors, the transverse confining potential usually looks more like that shown in Fig. 4.1.1a. In general, analytical solutions are not available for arbitrary confining potentials. However, there is an approximate solution that we can use at high magnetic fields. It is quite accurate if the cyclotron radius is small enough that the confining potential can be assumed to be nearly constant on this scale. Let us start by deriving this approximate result.

Magneto-electric subbands at high magnetic fields

We know that if the confining potential were absent ($U(y) = 0$) then the solutions to Eq.(4.1.1) would be given by (see Eqs.(1.6.8a,b))

$$\Psi_{n,k}(x,y) = \frac{1}{\sqrt{L}}\exp[ikx]u_n(q+q_k) \equiv |n,k\rangle \qquad (4.1.2)$$

$$E(n,k) = E_s + \left(n+\tfrac{1}{2}\right)\hbar\omega_c\,, \quad n = 0,1,2,\ldots$$

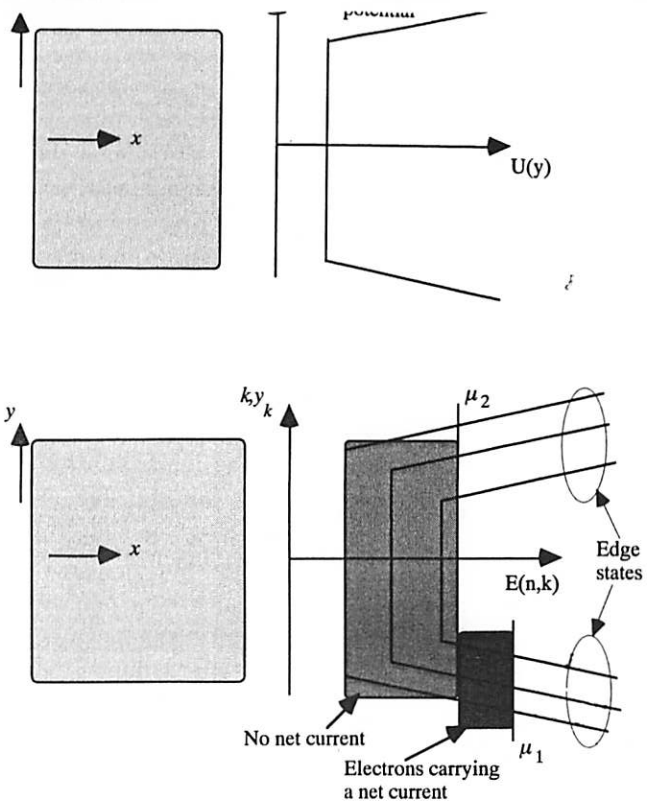

Fig. 4.1.1. A rectangular conductor assumed to be uniform in the x-direction. (*a*) Sketch of confining potential $U(y)$ versus y. (*b*) Sketch of the approximate dispersion relation assuming that the confining potential varies slowly over a cyclotron radius.

where $$u_n(q) = \exp\left[-q^2/2\right] H_n(q)$$

$$q = \sqrt{m\omega_c/\hbar}\, y \quad \text{and} \quad q_k = \sqrt{m\omega_c/\hbar}\, y_k$$

$$y_k \equiv \frac{\hbar k}{eB} \quad \text{and} \quad \omega_c \equiv \frac{|e|B}{m}$$

$H_n(q)$ is the nth Hermite polynomial.

Now let us use lowest order perturbation theory to include the effect of the confining potential $U(y)$:

$$E(n,k) \approx E_s + \left(n+\tfrac{1}{2}\right)\hbar\omega_c + \langle n,k|U(y)|n,k\rangle$$

in the transverse direction and has a spatial extent of $\sim(\hbar/m\omega_c)^{1/2}$. Assuming that the potential $U(y)$ is nearly constant over the extent of each state, we can write

$$E(n,k) \approx E_s + \left(n+\tfrac{1}{2}\right)\hbar\omega_c + U(y_k) \quad \text{where} \quad y_k = \hbar k/eB \qquad (4.1.3)$$

Figure 4.1.1b shows a sketch of the dispersion relation $E(n,k)$ vs. k. It looks just like the confining potential $U(y)$, with the coordinate y mapped onto the wavenumber k by the relation $y_k = \hbar k/eB$. In the middle of the sample the states look just like the Landau levels of an unconfined 2-D conductor spaced by $\hbar\omega_c$. Near the edges there are allowed states with a continuous distribution of energies. These are referred to as the edge states and they play a very important role in carrying the current at the resistance minimum.

What is the current carried by an edge state? From Eq.(4.1.3) we can calculate the velocity:

$$v(n,k) = \frac{1}{\hbar}\frac{\partial E(n,k)}{\partial k} = \frac{1}{\hbar}\frac{\partial U(y_k)}{\partial k} = \frac{1}{\hbar}\frac{\partial U(y)}{\partial y}\frac{\partial y_k}{\partial k} = \frac{1}{eB}\frac{\partial U(y)}{\partial y}$$

The edge states located at the two edges of the sample carry currents in opposite directions, since the quantity $\partial U(y)/\partial y$ changes sign. The bulk states too could carry current if there are electric fields in the interior of the sample due to, say, the Hall voltage. If $\mu_1 > \mu_2$ (as shown in Fig. 4.1.1) then the states below μ_2 are all filled (assuming 'zero' temperature) and essentially in equilibrium, so that they do not carry any net current. Any net current arises from the filled states between μ_1 and μ_2 (see Fig. 4.1.1b). The resistance of the sample is determined by the rate at which the electrons in these states can relax their momentum.

The situation is quite similar to that in an ordinary conductor carrying current. The positive k-states are occupied to a higher quasi-Fermi level than the negative k-states (see Fig. 1.7.2). The resistance at low temperatures is determined by the momentum relaxation time of the excess carriers in the positive k-states. What is unusual here is that the states carrying current in one direction are spatially separated from those carrying current in the opposite direction. To relax momentum an electron has to be scattered from the *left* of the sample to the *right* of the sample. This is all but impossible since the overlap between the wavefunctions is exponentially small and there are no allowed states in the interior of the sample in this energy range ($\mu_1 > E > \mu_2$).

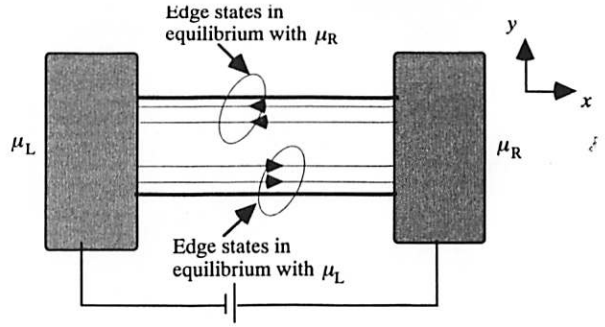

Fig. 4.1.2. A conductor in the quantum Hall regime. The edge states (two shown in the figure) carrying current to the right are in equilibrium with the left contact while those carrying current to the left are in equilibrium with the right contact.

As a result of this complete suppression of backscattering, electrons originating in the left contact enter the edge states carrying current to the right and empty into the right contact, while electrons in the right contact enter the edge states carrying current to the left and empty out into the left contact. Consequently, the edge states carrying current to the right are completely in equilibrium with the left contact and have a quasi-Fermi energy equal to μ_L. They are unaffected by μ_R since no electron originating in the right contact ever makes it to these states. Similarly we can argue that the edge states carrying current to the left all originate from the right contact and have a quasi-Fermi energy equal to μ_R (see Fig. 4.1.2):

$$\mu_1 = \mu_L \quad \text{and} \quad \mu_2 = \mu_R$$

Clearly the longitudinal voltage drop V_L as measured by two voltage probes located anywhere on the *same* side of the sample is zero, while the transverse (or Hall) voltage V_H measured by two probes located anywhere on *opposite* sides of the sample is equal to the applied voltage:

$$V_L = 0 \quad \text{and} \quad eV_H = \mu_L - \mu_R \tag{4.1.4a}$$

Note that this situation arises only when the electrochemical potentials lie between two bulk Landau levels. If the electrochemical potentials lie on a bulk Landau level then there is a continuous distribution of allowed states from one edge to the other. Electrons can scatter from the left of the sample to the right of the sample through the allowed energy states in the interior of the sample. This backscattering gives rise to a maximum in the longitudinal resistance every time [illegible] Landau level.

What is the current?

The current can be written down very simply by noting that the situation is very similar to what we had argued in Chapter 2 for a ballistic conductor (see Fig. 2.1.1). The number of edge states (which is equal to the number of filled Landau levels in the bulk) plays the role played by the number of modes in a ballistic conductor so that we can write (cf. Eq.(2.1.3))

$$I = \frac{2e}{h} M(\mu_L - \mu_R) \tag{4.1.4b}$$

We could derive this formally as follows (k_L and k_R are the wavenumbers corresponding to $E = \mu_L$ and $E = \mu_R$ respectively)

$$I = 2e\sum_n \int_{\mu_R}^{\mu_L} \frac{1}{2\pi} v(n,k)\mathrm{d}k = 2e\sum_n \int_{\mu_R}^{\mu_L} \frac{1}{2\pi}\frac{1}{\hbar}\frac{\partial E(n,k)}{\partial k}\mathrm{d}k$$

$$= \frac{2e}{h}\sum_n \int_{\mu_R}^{\mu_L} \mathrm{d}E = \frac{2e}{h} M\left[\mu_L - \mu_R\right]$$

Hence from Eqs.(4.1.4a, b) we can write down the longitudinal and Hall resistances:

$$R_L = \frac{V_L}{I} = 0 \quad \text{and} \quad R_H = \frac{V_H}{I} = \frac{h}{2e^2 M} \tag{4.1.5}$$

Note that a two-terminal resistance measurement would yield the Hall resistance. Only a four-terminal measurement with voltage probes located on the same side of the sample yields zero resistance.

Thus whenever the Fermi energy lies between two bulk Landau levels, the longitudinal resistance is very nearly zero and corresponding to the zeros in the longitudinal resistance, there appear plateaus in the Hall resistance (see Fig. 1.4.2). At these plateaus the Hall resistance has the value

$$R_H = \frac{h}{2e^2 M} = \frac{25.8128\,\mathrm{k\Omega}}{2M}$$

where M = number of edge states at the Fermi energy = number of bulk Landau levels below the Fermi energy. M takes on integer values that

striking accuracy (better than one part per million) of this quantization of R_H that is obtained at high magnetic fields. This phenomenon is known as the quantum Hall effect (or QHE) and was discovered in 1980. It is characteristic of 2-D semiconducting films and is not observed in bulk materials.

Note that the quantized Hall resistance has the same form as the quantized resistance of ballistic conductors (see Section 2.1) with the number of edge states playing the role of the number of modes. In ordinary ballistic conductors the quantization is not very precise because backscattering processes are not completely eliminated. But in the quantum Hall regime we have a ballistic conductor of incredibly high quality due to the spatial separation of the forward and the backward propagating states. As a result the quantization is extremely precise.

Application of the Büttiker formula

So far we have not worried explicitly about the voltage probes used to measure the longitudinal or the transverse voltage drops. We have assumed that such probes would measure the local quasi-Fermi energy for the corresponding edge states. The Büttiker formula discussed in Section 2.4 (see Eq.(2.4.4) or (2.5.8)) provides a natural framework for the analysis of multi-terminal conductors taking the probes explicitly into account. Both the zero longitudinal resistance and the quantized Hall resistance follow readily from the Büttiker formula, if we postulate that electrons can travel from one terminal to another without scattering. The transmission functions can be written down by inspection without any messy calculations of the type discussed in the last chapter. We will assume the bias and temperature to be low enough that the transmission function is essentially constant over the energy range where transport occurs. This allows us to use the linear response formula (Eq.(2.5.8)) without worrying about vertical flow (see Section 2.7).

Consider an ordinary macroscopic Hall bridge hundreds of microns in length and in width. We assume that electrons can travel from one terminal to another without momentum relaxation due to the formation of edge states. Since there is no backscattering, the transmission function $\bar{T}_{pq}$ is very easy to evaluate. We just have to count the number of current carrying channels that start from terminal p and end in terminal q. For the Hall bridge depicted in Fig. 4.1.3 having M (= 2 shown in the figure) edge states that carry current around the sample, it is evident that $\bar{T}_{pq} = M$

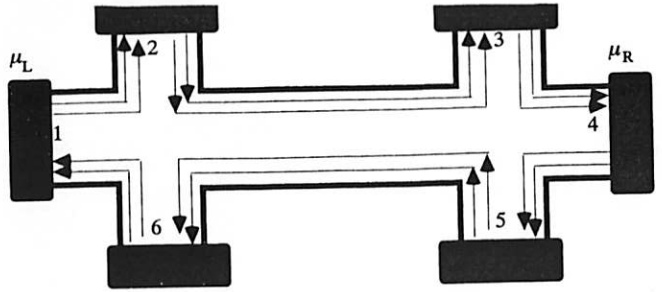

Fig. 4.1.3. Hall bridge at high magnetic fields showing two edge states at each edge.

only if (p←q) is equal to (1←6), (2←1), (3←2), (4←3), (5←4) or (6←5). All other transmission coefficients are zero. Neglecting any backscattering we can write down the conductance matrix (which is proportional to the transmission function) by inspection:

G_{pq}:	$q=1$	$q=2$	$q=3$	$q=4$	$q=5$	$q=6$
$p=1$	0	0	0	0	0	G_C
$p=2$	G_C	0	0	0	0	0
$p=3$	0	G_C	0	0	0	0
$p=4$	0	0	G_C	0	0	0
$p=5$	0	0	0	G_C	0	0
$p=6$	0	0	0	0	G_C	0

where $$G_C = \frac{2e^2 M}{h}$$

We can solve for the terminal currents and voltages starting from Eq.(2.5.8), which yields a system of six equations. As explained earlier (see discussion preceding Eq.(2.4.6)) these equations are not independent and we can choose the voltage at one of the terminals to be zero and omit the row and column corresponding to that terminal. Setting $V_4 = 0$,

$$\begin{Bmatrix} I_1 \\ I_2 \\ I_3 \\ I_5 \\ I_6 \end{Bmatrix} = \begin{bmatrix} G_C & 0 & 0 & 0 & -G_C \\ -G_C & G_C & 0 & 0 & 0 \\ 0 & -G_C & G_C & 0 & 0 \\ 0 & 0 & 0 & G_C & 0 \\ 0 & 0 & 0 & -G_C & G_C \end{bmatrix} \begin{Bmatrix} V_1 \\ V_2 \\ V_3 \\ V_5 \\ V_6 \end{Bmatrix}$$

necessary. We can easily write down the solution to the above set of equations noting that the currents at the voltage terminals are all zero ($I_2 = I_3 = I_5 = I_6 = 0$):

$$V_2 = V_3 = V_1, \quad V_5 = V_6 = 0$$

This is of course precisely what we had assumed, namely, that any voltage probe on one side floats to a potential equal to the right contact while any probe on the other side floats to a potential equal to the left contact. Also the current is given by

$$I_1 = G_C V_1$$

so that the longitudinal resistance R_L measured between probes 2 and 3 or between 5 and 6 is zero

$$R_L = \frac{V_2 - V_3}{I_1} = \frac{V_6 - V_5}{I_1} = 0$$

while the Hall resistance R_H measured between probes 2 and 6 or between 3 and 5 has the quantized value stated earlier (see Eq.(4.1.5)).

$$R_H = \frac{V_2 - V_6}{I_1} = \frac{V_3 - V_5}{I_1} = G_C$$

Does the current flow only at the edges?

We stated above that if $\mu_1 > \mu_2$ (as shown in Fig. 4.1.1) then the states below μ_2 are all filled and do not carry any net current. Any net current can be calculated from the filled states on the left between μ_1 and μ_2. However, this does not mean that current flows only near the edge having the potential μ_1. There are currents everywhere in the sample. We could choose to do our bookkeeping in a different way so that the net current appears at a different spatial location. We have identified all the states below μ_2 (note that $\mu_1 > \mu_2$) as our Fermi sea which does not carry any net current. Consequently the net current is carried by electrons in the edge states on one side of the sample with energies lying in the range $\mu_1 > E > \mu_2$. But we could just as well identify all the states below μ_1 as our Fermi sea. The net current would then be carried by the *holes* occupying the edge states on the *other side* of the sample!

We mentioned in Section 1.7 that while the *conductance* at low temperatures is a [illegible] quantum Hall conductor provides a very good example of this. At low temperatures the current is carried by the states near the Fermi energy. States lying deep inside the Fermi sea have no effect on the conductance. But the local current density due to these states is not zero. These states give rise to circulating currents in the sample even at equilibrium. An applied electric field can induce a change in this circulating current flow pattern thus contributing to the conductivity tensor defined by the relation $\delta\mathbf{J} = \sigma\delta\mathbf{E}$. Thus electrons deep inside the Fermi sea can contribute to the conductivity, even though they do not contribute to the conductance.

Why should the Fermi energy ever lie between Landau levels?

The above discussion shows that the longitudinal resistance can be extremely small if the electrochemical potentials μ_1 and μ_2 were located between bulk Landau levels as shown in Fig. 4.1.1. This requires that the equilibrium Fermi energy E_f must be located between the Landau levels since at low bias $\mu_1 \sim \mu_2 \sim E_f$. How is the location of E_f determined?

At low temperatures we can write

$$n_s = \int_{-\infty}^{E_f} N_s(E,B)\mathrm{d}E$$

where n_s is the electron density and N_s is the density of states. The electron density increases with the Fermi energy as shown in Fig. 4.1.4. The important point to note is that the electron density increases rapidly whenever the density of states is high. This is because a change in the electron density is related to the change in the Fermi energy by the relation

$$\delta n_s = N_s(E_f, B)\delta E_f$$

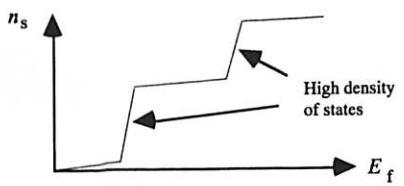

Fig. 4.1.4. Electron density vs. Fermi energy. Note that the electron density changes rapidly whenever the density of states is high.

region where the density of states N_s is very small. A slight change in the electron density would cause a large shift in the Fermi energy. The Fermi energy thus tends to be *pinned* to energies where the density of states is high.

From this point of view we would expect the the Fermi energy to be pinned to one Landau level or another, where the density of states is high. If this were true then the low resistance condition discussed earlier would never be observed since the Fermi energy would never be located between two Landau levels. This is not a problem in narrow conductors where the edge states provide a significant density of states between the Landau levels. But in wide conductors the edge states represent a negligible fraction of the total density of states. How can the Fermi energy in a wide conductor ever lie between the bulk Landau levels, leading to the low resistance condition that we have been discussing?

It is believed that in practice the density of states between two Landau levels is quite significant because real samples have potential fluctuations leading to the formation of localized states (see for example the introductory article in Ref.[4.3] by Prange). This can be understood by noting that potential fluctuations in the interior of the sample lead to the formation of local equipotential contours that close on themselves as shown in Fig. 4.1.5a. Since cyclotron orbits drift along equipotential contours they get stuck at these spots forming localized states. These states do not contribute to the current flow but they help stabilize the Fermi energy between Landau levels by providing a respectable density of states between Landau levels as sketched in Fig. 4.1.5b.

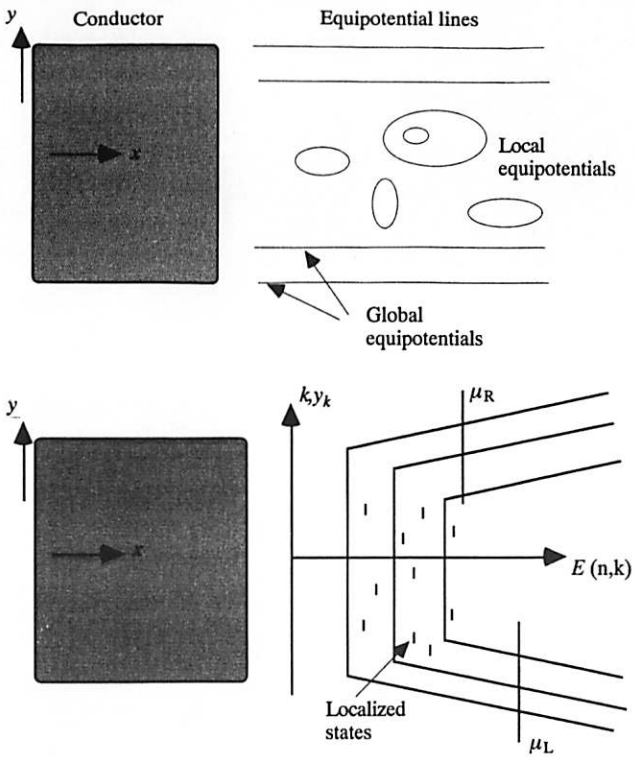

Fig. 4.1.5. (*a*) Potential fluctuations in the interior of the sample lead to local equipotentials where cyclotron orbits get stuck forming localized states. (*b*) These localized states help stabilize the Fermi energy between Landau levels.

Fractional quantum Hall effect

We have seen that in the quantum Hall regime the Hall resistance takes on quantized values given by

$$\rho_{yx} = \frac{h}{2e^2 M} = \frac{25.8128\,\text{k}\Omega}{2M}$$

where M is an integer. Actually at high fields the energy levels for the two spins split apart due to the Zeeman effect and quantized plateaus are obtained with

$$\rho_{yx} = \frac{h}{e^2 M} = \frac{25.8128\,\text{k}\Omega}{M}$$

When the magnetic field reaches a value such that the electron density $n_s = eB/h$, we will have all the electrons in a single Landau level with one spin. For a carrier density of $n_s = 2 \times 10^{11}/\text{cm}^2$, this requires a field of about 8 T. What happens if we increase the field further?

From our earlier discussion we might expect that there will be no further plateaus with increasing magnetic field since the Fermi energy now lies in the middle of a Landau level (the last!). Experimentally, however, in very pure samples one continues to observe plateaus in the Hall resistivity given by

$$\rho_{yx} = \frac{h}{e^2 p} = \frac{25.8128\,\text{k}\Omega}{p}$$

where p is a rational fraction like $\frac{1}{3}, \frac{2}{5}, \frac{4}{7}$ etc. This is referred to as the

integral quantum Hall effect (or IQHE) that we have been discussing. The FQHE arises from the formation of a novel many-body ground state (see R. B. Laughlin (1983), *Phys. Rev. Lett.* **50**, 1395) whose quasiparticle excitations are very different from what we expect from the simple one-particle picture that we have been using to describe the IQHE. We refer the reader to the references cited at the end of this chapter and also to the book by T. Chakraborty and P. Pietilainen (1988), *The Fractional Quantum Hall Effect*, (New York, Berlin, Heidelberg, Springer-Verlag).

4.2 Effect of backscattering

So far we have assumed that there is no backscattering so that each edge state has a transmission probability of 100%. Once we make this assumption, zero longitudinal resistance and the quantized Hall resistance follow naturally from the Landauer–Büttiker formalism. However, the real power of this formalism lies in providing a clear description of the many experiments in the quantum Hall regime reported in the late 1980s where controlled amounts of backscattering are deliberately introduced. Indeed this is one of the most elegant applications of the Landauer–Büttiker formalism.

Suppose a split gate is used to pinch off the Hall bar (between probes 2 and 3, see Fig. 4.2.1) so that only N ($N < M$) edge channels can propagate through the constriction, then the remaining $(M - N)$ channels will be completely backscattered. The net current from left to right is given by

$$I_1 = \frac{2e}{h}N(\mu_L - \mu_R) = \frac{2e^2}{h}NV_1 \quad \text{(setting } \mu_L = eV_1 \text{ and } \mu_R = 0\text{)}$$

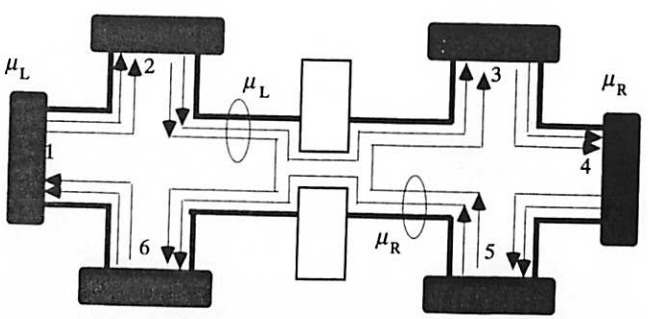

Fig. 4.2.1. Hall bridge with split gate structure used to backscatter one edge channel while the other can transmit.

There is an optical analogues for such a system.

We can write the current as

$$I_1 = \frac{2e^2}{h}MV_1(1 - p)$$

where $$p \equiv \frac{M - N}{M} = \frac{\text{No. of backscattered channels}}{\text{Total no. of channels}}$$

The contact 2 'sees' only the channels originating from the left having a potential μ_L, while the contact 5 'sees' only the channels originating from the right having a potential μ_R.

$$\mu_2 = eV_1 \quad \text{and} \quad \mu_5 = 0$$

The contact 6 'sees' $(M - N)$ channels that originate from the left and have a potential μ_L and N channels that originate from the right and have a potential μ_R. Consequently it floats to a potential of

$$\mu_6 = \frac{(M - N)\mu_L + N\mu_R}{M} = eV_1 p$$

Similarly the potential at contact 3 is given by

$$\mu_3 = \frac{N\mu_L + (M - N)\mu_R}{M} = eV_1(1 - p)$$

Hence the longitudinal resistance R_L measured between probes 2 and 3 or between 5 and 6 is given by

$$R_L = \frac{V_1 p}{I_1} = \frac{h}{2e^2 M}\left[\frac{p}{1-p}\right] = \frac{h}{2e^2}\left[\frac{1}{N} - \frac{1}{M}\right] \qquad (4.2.1)$$

This 'fractional quantization' of the longitudinal resistance has been observed experimentally. The Hall resistance R_H measured between probes 2 and 6 or between 3 and 5 is unchanged from its usual quantized value:

$$R_H = \frac{V_1(1-p)}{I_1} = \frac{h}{2e^2 M} \qquad (4.2.2)$$

Application of the Büttiker formula

The above results follow quite readily from the Büttiker formula which takes the voltage probes explicitly into account. The conductance matrix can be written as

	$q=1$	$q=2$	$q=3$	$q=4$	$q=5$	$q=6$
$p=1$	0	0	0	0	0	G_C
$p=2$	G_C	0	0	0	0	0
$p=3$	0	$(1-p)G_C$	0	0	pG_C	0
$p=4$	0	0	G_C	0	0	0
$p=5$	0	0	0	G_C	0	0
$p=6$	0	pG_C	0	0	$(1-p)G_C$	0

Hence from Eq.(2.5.8) (setting $V_4 = 0$ and leaving out the rows and columns corresponding to terminal 4 as we did before)

$$\begin{Bmatrix} I_1 \\ I_2 \\ I_3 \\ I_5 \\ I_6 \end{Bmatrix} = \begin{bmatrix} G_C & 0 & 0 & 0 & -G_C \\ -G_C & G_C & 0 & 0 & 0 \\ 0 & -(1-p)G_C & G_C & -pG_C & 0 \\ 0 & 0 & 0 & G_C & 0 \\ 0 & -pG_C & 0 & -(1-p)G_C & G_C \end{bmatrix} \begin{Bmatrix} V_1 \\ V_2 \\ V_3 \\ V_5 \\ V_6 \end{Bmatrix}$$

As before it is straightforward to write down the solution, noting that the currents at the voltage terminals are all zero ($I_2 = I_3 = I_5 = I_6 = 0$):

$$V_2 = V_1, \quad V_5 = 0, \quad V_3 = (1-p)V_1, \quad V_6 = pV_1$$

and

$$I_1 = G_C(1-p)V_1$$

Eqs.(4.2.1) and (4.2.2) follow readily, noting that

$$R_L = \frac{V_2 - V_3}{I_1} = \frac{V_6 - V_5}{I_1}$$

$$R_H = \frac{V_2 - V_6}{I_1} = \frac{V_3 - V_5}{I_1}$$

Disordered contacts

The fact that the Hall resistance is unaffected by the backscattering (see Eq.(4.2.2)) may seem obvious. After all, contacts 2 and 6 are located hundreds of microns away from the split-gate scatterers. Surely the effect of the scatterers cannot be felt so far away! However, experimentally it has been observed that often the Hall resistance too is affected by the split gates. This can be understood if we postulate that there is no communication among the edge states on the *same side* of the sample and the contacts do not communicate equally with all the edge states. For example, suppose there is a defect or an impurity near contact 6 such that it only 'sees' the outer edge states and the remaining edge states bypass it and go directly to contact 1 (see Fig. 4.2.2).

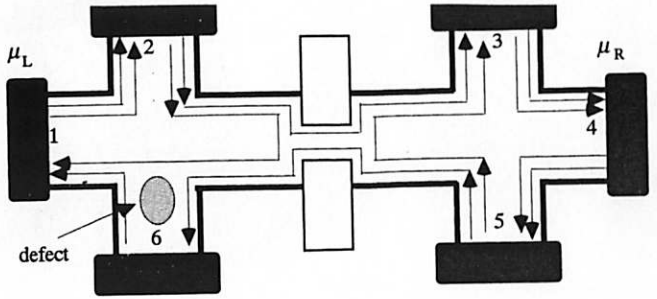

Fig. 4.2.2. Same as Fig. 4.2.1 but with contact 6 'disordered'.

We would then expect contact 6 to float to a potential equal to $\mu_R = 0$, instead of eV_1p as we had reasoned earlier. Consequently the measured Hall resistance is given by

$$\frac{V_2 - V_6}{I_1} = \frac{V_1}{I_1} = \frac{h}{2e^2M}\frac{1}{1-p} \quad \text{instead of} \quad \frac{h}{2e^2M}$$

and is affected by the presence of the split-gate structure through the factor p. Note that this is only true if the edge states on the same side of the sample do not communicate with each other. If they do communicate, then they will tend to equilibrate and thereby acquire a common average potential equal to $eV_1(1-p)$. Even if contact 6 'sees' only one of the edge states it will register this average potential, so that the measured Hall resistance will be independent of p. The fact that the measured Hall resistance is affected by the split gate shows that there is lack of equilibration between edge states on the same side of the sample. These results (as well as those for other types of disordered contacts) can be obtained readily from the Büttiker formula, as shown in Exercises E.4.1 and E.4.2 at the end of this chapter (see also Refs.[4.1], [4.2]).

Non-ohmic behavior of R_L

We know that when the Fermi energy lies on a bulk Landau level, the edge states are backscattered through the bulk level to a state on the

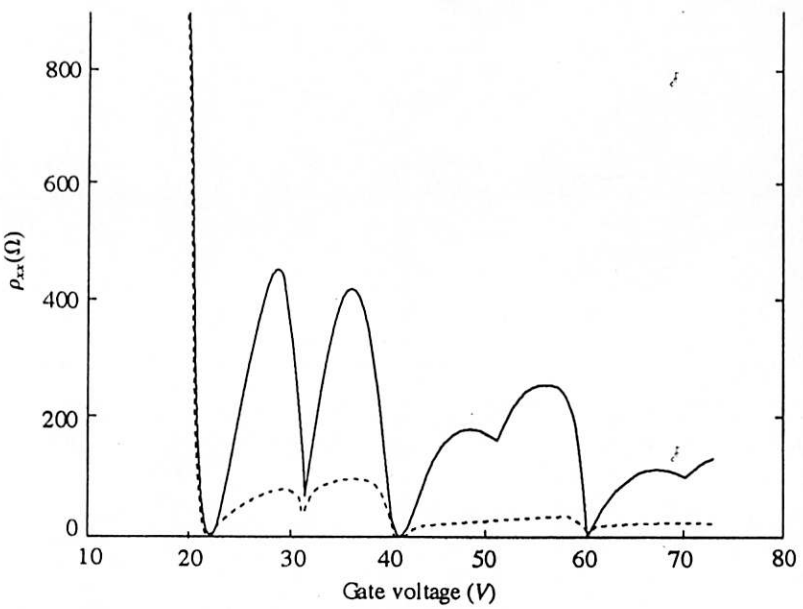

Fig. 4.2.3. Measured resistivity in two silicon field-effect transistors at a magnetic field of $B = 12$ T as a function of the gate voltage (which changes the carrier concentration). The two structures are identical and have the same width $W = 40$ μm. The only difference is the distance between the voltage probes: it is 80 μm for one sample and 2880 μm for the other. The resistivity ρ_{xx} is deduced from the measured resistance assuming the ohmic scaling law. The strong discrepancy between the resistivities in the two samples shows the breakdown of ohmic scaling. The discrepancy goes away above 4 K. Reproduced with permission from Fig. 2 of R. J. Haug and K. von Klitzing (1989), *Europhys. Lett.*, **10**, 489–92.

other side giving rise to a longitudinal resistance. These are the peaks in the SdH oscillations as discussed in Section 1.5. We would expect this peak resistance to scale linearly with the spacing between the voltage probes in accordance with Ohm's law. Experimentally it has been shown that the resistance does not increase linearly (see Fig. 4.2.3).

This non-ohmic behavior can be understood if we postulate that at high fields (when the Fermi energy lies on a bulk Landau level), it is only the innermost edge state that is backscattered through the bulk level to a state on the other side. The remaining edge states can still propagate hundreds of microns without backscattering. As a result when we make the distance between two voltage probes longer and longer, the net backscattering in the region between them does not increase asymptotically to one. Thus the longitudinal resistance measured between two voltage probes does not increase linearly with the [illegible] expected from Ohm's law. Instead it saturates to a maximum value of (see Eq.(4.2.1) with $N = M - 1$)

$$R_L(\text{maximum}) = \frac{h}{2e^2}\left(\frac{1}{M-1} - \frac{1}{M}\right)$$

If we assume ohmic scaling and divide the measured resistance by the probe spacing to obtain the resistivity, then samples with larger probe spacing will yield smaller resistivity values as observed experimentally (see Fig. 4.2.3).

It is really quite surprising that states on the same side of the sample can travel such huge distances (1000 μm is actually 1 mm and is clearly visible to the naked eye) without equilibration. This means that even a sample 1 mm long may exhibit mesoscopic behavior. A number of experiments have been reported by different groups that support this observation (see, for example, P. L. McEuen *et al.* (1991), *Phys. Rev. Lett*, **64**, 2062).

Summary

In a two-dimensional conductor at high magnetic fields, the states carrying current in opposite directions are located on opposite sides of the sample. If the Fermi energy lies between two bulk Landau levels then the states (at the Fermi energy) are completely decoupled from each other (see Fig. 4.1.1). This leads to a complete suppression of backscattering processes resulting in a perfectly ballistic conductor. The longitudinal resistance measured with two probes placed along an edge is zero while the Hall resistance measured with two probes on opposite sides of the sample is quantized in units of $(h/2e^2)$ with an impressive accuracy that is specified in parts per million (Section 4.1). In this quantum Hall regime even conductors with dimensions of the order of millimeters exhibit 'mesoscopic' phenomena that cannot be described in terms of a conductivity tensor. For example, the longitudinal resistance does not scale linearly with length according to Ohm's law (see Fig. 4.2.3); measurements can be affected by the mere presence of a floating probe even if it is not used (see Exercise E.4.2); etc. The Landauer–Büttiker formalism provides a simple framework for the description of such phenomena.

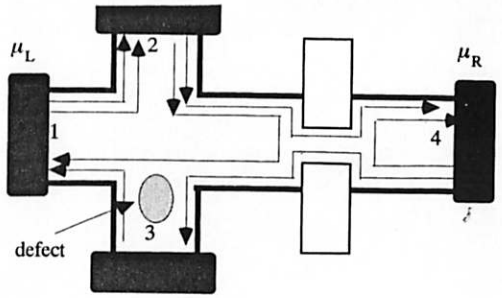

Fig. E.4.1. Same as in Fig. 4.2.2 but with terminals '3' and '5' omitted and terminal '6' renumbered as '3'.

Exercises

E.4.1 Consider a slightly simplified form of the structure shown in Fig. 4.2.2, as shown in Fig. E.4.1.

(a) Write down the conductance matrix for this structure assuming that there is no communication between edge states as they propagate from the constriction to terminal 3.

(b) Use the Büttiker formula (Eq.(2.5.8)) to show that the Hall resistance is given by

$$R_H = \frac{V_2 - V_3}{I} = \frac{h}{2e^2 M}\frac{1}{1-p}$$

as reasoned in the text.

E.4.2 Consider the same structure as in E.4.1 but with an extra terminal '5' inserted, as shown in Fig. E.4.2.

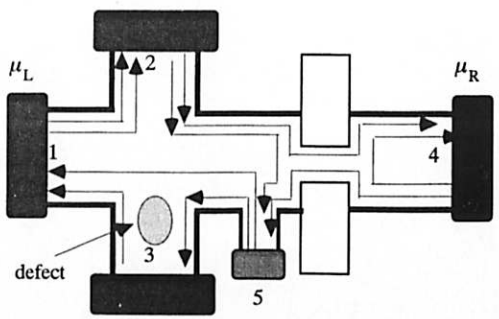

Fig. E.4.2. Same as in Fig. E.4.1 but with an extra terminal '5' inserted.

Write down the conductance matrix for this structure and show that the Hall resistance is now given by

$$R_H = \frac{V_2 - V_3}{I} = \frac{h}{2e^2 M}$$

The extra terminal establishes equilibrium between the edge states and changes the Hall resistance. This is a rather surprising result which has been observed experimentally. In macroscopic conductors, we do not expect an extra floating probe ('5') to affect the measurement.

Further reading

A detailed review of the work in the late 1980s applying the Landauer–Büttiker formalism to the quantum Hall regime can be found in

[4.1] Beenakker, C. W. J. and van Houten, H. (1991), 'Quantum transport in semiconductor nanostructures' in *Solid State Physics*, vol.44, eds. H. Ehrenreich and D. Turnbull (New York, Academic Press) (see part IV).

[4.2] Büttiker, M. (1991). Chapter in *Nanostructured Systems*, ed. M. Reed, *Semiconductor and Semimetals*, vol.35, p.191.

A discussion of the earlier work on the quantum Hall effect (integer and fractional) can be found in

[4.3] Prange, R. E. and Girvin, S. M. (1987), eds. *The Quantum Hall Effect*, (New York, Springer).

[4.4] Chakraborty, T. (1992), 'The quantum Hall effect', in *Handbook on Semiconductors*, Chapter 19, ed. P. T. Landsberg (Amsterdam, New York, Oxford, North-Holland).

But $$\left[E - H + i\eta\right]_{-B}\left[G^{K}\right]_{-B} = I$$

Hence $$\left[G^{R}\right]_{-B} = \left[G^{A}\right]^{*}_{+B}$$

Since the advanced function is the conjugate transpose of the retarded function we obtain the desired result ('t' denotes transpose):

$$\left[G^{R}\right]_{-B} = \left[G^{R}\right]^{t}_{+B}$$

From Eq.(3.4.6) (assuming zero magnetic field in the leads)

$$\begin{aligned}\left[s_{nm}\right]_{-B} &= -\delta_{nm} + i\hbar\sqrt{v_n v_m}\iint \chi_n(y_q)\left[G^{R}_{qp}(y_q;y_p)\right]_{-B}\chi_m(y_p)dy_q dy_p \\ &= -\delta_{mn} + i\hbar\sqrt{v_m v_n}\iint \chi_m(y_p)\left[G^{R}_{pq}(y_p;y_q)\right]_{+B}\chi_n(y_q)dy_q dy_p \\ &= \left[s_{mn}\right]_{+B}\end{aligned}$$

Chapter 4

E.4.1 (a)

G_{pq}:	$q=1$	$q=2$	$q=3$	$q=4$
$p=1$	0	pG_C	$(1-p)G_C$	0
$p=2$	G_C	0	0	0
$p=3$	0	0	pG_C	$(1-p)G_C$
$p=4$	0	$(1-p)G_C$	0	pG_C

Note that we have written $G_{33} = pG_C$ in order to have all the sums and columns add up to the same number G_C, assuming all leads to have the same number of modes. However, the actual currents are unaffected by what we choose for the diagonal elements of G_{pq}.

(b)

$$I_2 = 0: \qquad V_2 = V_1$$
$$I_3 = 0: \qquad V_3 = V_4$$

$$I_1 = I = pG_C(V_1 - V_2) + (1-p)G_C(V_1 - V_3) = (1-p)G_C(V_2 - V_3)$$

Hence $$R_H = \frac{V_2 - V_3}{I_1} = \frac{1}{G_C}\frac{1}{1-p}$$

E.4.2

G_{pq}:	$q=1$	$q=2$	$q=3$	$q=4$	$q=5$
$p=1$	0	0	$(1-p)G_C$	0	pG_C
$p=2$	G_C	0	0	0	0
$p=3$	0	0	pG_C	0	$(1-p)G_C$
$p=4$	0	$(1-p)G_C$	0	pG_C	0
$p=5$	0	pG_C	0	$(1-p)G_C$	0

Setting $V_4 = 0$,

$$I_2 = 0: \qquad V_2 = V_1$$
$$I_3 = 0: \qquad V_3 = V_5$$
$$I_5 = 0 = p(V_5 - V_2) + (1-p)(V_5 - V_4) \qquad V_5 = pV_2$$
$$I_1 = I = pG_C(V_1 - V_5) + (1-p)G_C(V_1 - V_3) = G_C(V_1 - V_5)$$

Hence $$R_H = \frac{V_2 - V_3}{I_1} = \frac{1}{G_C}$$

Chapter 5

E.5.1 $$\mathbf{J} = -\sigma\nabla\varphi, \quad \nabla\cdot\mathbf{J} = 0 \;\rightarrow\; \nabla^2\varphi = 0$$

In a circular geometry we can write

$$\varphi(\mathbf{r}) = \frac{-V\ln(r/L_{min})}{\ln(L_{max}/L_{min})} \;\rightarrow\; \mathbf{E}(\mathbf{r}) = \hat{r}\frac{V/r}{\ln(L_{max}/L_{min})}$$

Hence $$\mathbf{J}(\mathbf{r}) = \hat{r}\frac{\sigma V/r}{\ln(L_{max}/L_{min})}$$

so that the net current is given by

$$I = \int \mathbf{J}\cdot d\mathbf{S} = \frac{\pi\sigma V}{\ln(L_{max}/L_{min})} \;\rightarrow\; G = \frac{I}{V} = \frac{\pi\sigma}{\ln(L_{max}/L_{min})}$$

E.5.2 We can write Eq.(5.5.30) in the form

$$\frac{-\Delta\sigma}{e^2/\pi h} = \left[\Psi\left(\frac{1}{2} + \frac{B_m}{B}\right) - \Psi\left(\frac{1}{2} + \frac{B_\varphi}{B}\right)\right]$$